Modeling of Scalar Dependencies of Soft Magnetic Material Magnetization for Electrical Machine Finite-Element Simulation

Xiao Xiao[1], Fabian Müller[1], Gregor Bavendiek[1], Nora Leuning[1], Pengfei Zhang[2], Jun Zou[2], and Kay Hameyer[1]

[1]Institute of Electrical Machines (IEM), RWTH Aachen University, 52056 Aachen, Germany
[2]State Key Laboratory of Power System, Department of Electrical Engineering, Tsinghua University, Beijing 100084, China

The magnetization behavior and thus the form of the magnetization curve of electrical steel strongly depend on the direction of the magnetic field, frequency of excitation, external mechanical stress, and cut edge effect. These factors influence the performance of electrical machines and need to be considered in advanced machine design processes or numerical modeling. Most of the aforementioned effects occur locally in the machine and, therefore, need to be described locally. It is crucial to characterize the material under realistic conditions for adequate identification and quantification of the influences. In this article, modeling and simulation of soft magnetic material are performed based on a detailed magnetic characterization, considering magnetization amplitude, angle with respect to the rolling direction of magnetization, mechanical stress, and cut edge effect. The dependent soft magnetic material characteristics are derived from the magnetic measurement data and concluded into interpolation surfaces. Subsequently, these surfaces are used to simulate a synchronous machine designed for a traction drive of an electric vehicle by finite-element simulation. One of the main challenges is the correct determination of the local material properties, depending on the operating point, which influences global quantities such as losses and torque. This article provides a methodology to consider different local influences on the magnetization behavior of electrical steel in a finite-element simulation, thus offering the potential for improving electromagnetic circuit design.

Index Terms— **Electromagnetic measurements, electromagnetic modeling, finite-element analysis, material properties, soft magnetic material.**

I. Introduction

THE designs of wide-range applicable electrical machines require accurate knowledge of the soft magnetic material properties. The production process of nonoriented (NO) electrical steel sheets leads to an anisotropy of magnetic properties. Crystallographic texture and residual stress from the rolling process are sources of the anisotropy [1]. As a result, even NO materials possess a preferred direction of magnetization [2]. The processing from electrical steel sheets to motor laminations, for example, by shear cutting, induces plastic deformation as well as residual stress in the materials, which leads to the so-called cut edge effect. The effect describes the decrease of permeability in the vicinity of the cut edge which essentially decreases the magnetizability [3], [4]. Motor laminations are then stacked, packaged, and fitted into a housing to form the magnetic core. Furthermore, a high mechanical centrifugal force during the operation of the machines leads to additional mechanical stress contributions. All of the mentioned production and processing influences alter the magnetization behavior of NO materials, mainly due to the mechanical stress [5]. Hence, using regular magnetization curves obtained from unprocessed sheet material in finite-element (FE) simulations will lead to inaccurate results, although there is usually a compensation in the post-processing by calculating the iron losses. In this article, a material simulation model, which includes the dependence on mechanical stress, cut edge effect, and magnetic anisotropy, is implemented in order to improve the accuracy of machine design. The error from the simulation with one single nonlinear magnetization curve compared with the simulation results considering the applied dependencies locally in each element is examined in detail. Although this article focuses on the magnetization curve, the presented methodology is adaptable to the anhysteretic curve of hysteresis models. In this article, the required magnetic measurements for the identification routines and database are presented and the applied material models for the effects are derived. A comparison of magnetization properties from the material models to the measurements is given. The influence of magnetic materials under different dependencies on electrical machines is discussed by the results of the FE simulation.

II. Processing of Material Measurements

In this article, the magnetization behavior of an industrial NO M300-35A electrical steel is performed on a standard uniaxial single-sheet tester (SST). The different magnetic characterization conditions are collected in Table I. The samples are excited from a sinusoidal unidirectional magnetic-flux density of 0.1–1.8 T in steps of 0.1 T. To account for the material saturation polarization, an extrapolation to higher polarizations up to 2.03 T is used. The measurements are performed at the excitation frequency of 50 Hz. Due to the SST setup, the sample can only be excited in one direction. The magnetic-field strength and magnetic polarization are considered to be parallel. In order to determine the anisotropic properties,

Manuscript received August 18, 2019; revised October 7, 2019; accepted October 21, 2019. Date of current version January 20, 2020. Corresponding author: X. Xiao (e-mail: xiao.xiao@iem.rwth-aachen.de).

Color versions of one or more of the figures in this article are available online at http://ieeexplore.ieee.org.

Digital Object Identifier 10.1109/TMAG.2019.2950527

TABLE I
MEASURING PROCEDURE

dependencies	measurements
stresses (1 sample)	-8MPa, -4MPa, -3MPa, 0MPa, 3MPa, 5MPa, 10MPa, 15MPa, 20MPa, 25MPa
cut edge (5 samples)	60mm, 30mm, 15mm, 7.5mm, 5mm
directions (16 samples)	0°, 5°, 10°, 15°, 20°, 25°, 30°, 35°, 45°, 60°, 65°, 70° 75°, 80°, 85°, 90°

sample cuts of an angle from 0° to 90° relative to the rolling direction are used. In this way, the magnetization properties in each direction can be obtained with SST. With the help of equipping a hydraulic pressure cylinder with the SST, the stress response of the material can be obtained. A maximum tensile or compressive force of 5 kN can be applied. The applied stress is collinear to the magnetic field. The sample for stress measurements has a length of 600 mm and a width of 100 mm. In this article, the measured range is limited from −8 to 25 MPa. In order to simulate the magnetic field to be dependent on a wider range of stresses in electric machines, a stress model based on these measurements is required to be built for ±400 MPa. To characterize the cut edge effect, a set of electrical steel samples of 120 mm × 120 mm is cut into N strips with according widths of 120 mm × 120 mm/N as in [6] as to increase the proportion of cut surface per fixed sample volume. For instance, a sample with $N = 8$, is composed of eight strips of 15 mm width. The specimens that are cut are stacked together to form a full sample of 120 mm × 120 mm and are then measured with the help of SST.

III. MATERIAL MODELING APPROACHES

As presented in Section II, the measurements cannot be performed up to saturation or carried out in a continuous database considering various dependent parameters. For this reason, continuous material models are implemented to represent the relationship of $J(H, \sigma)$, $J(H, x)$, and $J(H, \theta)$. In order to examine the local permeability during the simulation, these material models have been integrated into a FE solver. The polarization of each material model is extrapolated to 2.03 T, which are depicted later in the figures of magnetization surfaces. Then, the local relationship between B and H can be obtained from these surfaces.

A. Stress Consideration

Considering the machine construction and operation conditions, the rotor lamination bears compressive stress up to −70 MPa, due to the assembly process, and at the same time centrifugal tensile stress up to 400 MPa. Different models have been published, representing locally magnetic behavior according to stress distribution in electric machines [7], [8]. Here it is assumed that the polarization is degraded symmetrically and quadratically in tensile and compressed direction. With this assumption, $J(H, \sigma)$ is interpolated from the measurements and extrapolated to the range of ±400 MPa as shown in Fig. 1. To simulate the stress-dependent magnetic field, the simulation model should at first be calculated in a mechanical solver while considering the assembly and operating point in order to assign each element to certain stress. Afterward, with the polarization surface, the magnetization curve for each element can be determined during the FE simulation of electromagnetic fields.

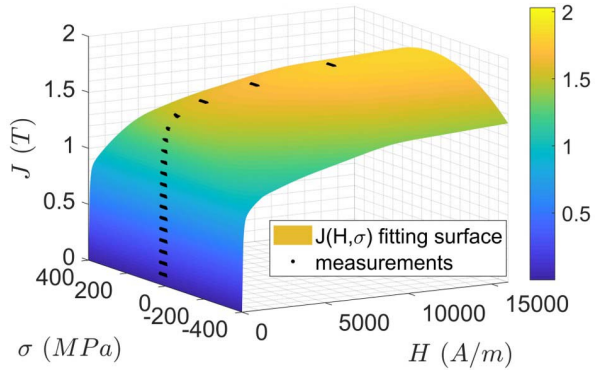

Fig. 1. Polarization in dependence with stresses and magnetic-field strength.

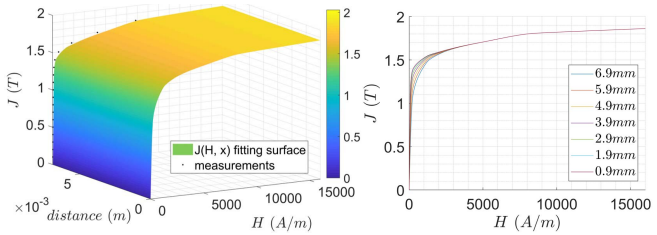

Fig. 2. Magnetization properties affected by cut edge effect. (a) $J(H,$ width). (b) $J(H, x)$.

B. Cut Edge Consideration

Fig. 2(a) shows that the magnetic polarization curve decreased with narrower strips. Several cutting edge modeling approaches are presented in [9] and [10]. The cut edge model here represents magnetization properties in a relationship with distance x to the cutting edge

$$\mu_r(H, x) = \mu_r(H, N = 0) - \Delta\mu_{\text{cut}}(H) \cdot \eta(x) \tag{1}$$

$\mu_r(H, N = 0)$ represents the undamaged permeability from the sample with a size of 120 mm × 120 mm. $\eta(x)$ is the degradation profile corresponding to x. It takes the influence from the depth of the sample and slope of deterioration into account. For the material sample used in this article, it turns out to be $\eta(x = 6.32 \text{ mm}) = 0$. This means that the permeability of the position with a distance to cut edge exceeding 6.32 mm should be equal to $\mu_r(H, N = 0)$, as the undamaged specimen [shown in Fig. 2(b)]. $\Delta\mu_{\text{cut}}(H)$ is the maximum change between permeability from undamaged specimens and specimens with different widths of cutting strips, which describes the relationship between permeability, distance to cut edge, and strip width. With algorithms, assigning each element a distance to the cut edge, the $J(H, x)$ relationship in Fig. 2(b) can be applied to the FE-solver to examine the local magnetization behavior of each element.

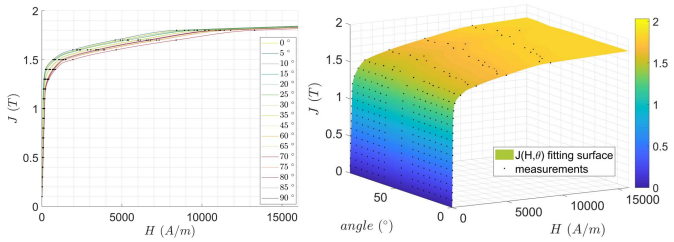

Fig. 3. Polarization in different angles relative to rolling direction. (a) $J(H, \theta)$ in 2-D. (b) $J(H, \theta)$ surface.

C. Anisotropy Consideration

Besides the cut edge effect on the magnetizability during the production of electromagnetic sheets, anisotropy is another phenomenon that appears through mechanical deformation. To achieve a certain polarization in different excitation directions, different magnetic-field strengths are required. Fig. 3(a) reveals the magnetization behavior by interpolating the measured data from the rolling to the transverse direction in 2-D. At lower polarization, the anisotropy is induced from domain wall pinning, which is decided by a microstructure of the material [11], [12]. From 1.4 to 1.8 T, the magnetization differs from each direction conspicuously. In this range, the magnetizing is caused predominantly by domain rotation. The domains quickly align along the external field in the magnetic easy direction and slowly in the hard direction. In this hard direction, with an angle of 70° to the rolling direction, the material is most difficult to be magnetized than that in other directions. By increasing the magnetic-field strength, the anisotropic characteristic vanishes by saturation. Fig. 3(b) shows the polarization surface in relation to magnetic-field strength and excitation direction. With $J(H, \theta)$, it is also able to simulate the vector anisotropy of the material [13].

IV. Nonlinear Finite-Element Model

Consecutive to the modeling of the different nonlinear material characteristic in electrical machines, the finite-element method (FEM) in combination with the magnetic vector potential formulation is employed. The magnetoquasi-static formulation of the FEM originates from the Ampère law, which describes that the rotation of **H** is equal to the current density

$$\nabla \times \nu(\nabla \times \boldsymbol{A}) + \sigma \frac{\mathrm{d}\boldsymbol{A}}{\mathrm{d}t} = \boldsymbol{J} \tag{2}$$

$$\boldsymbol{B} = \nabla \times \boldsymbol{A}. \tag{3}$$

J represents the current density, **B** is the magnetic-flux density, and **A** is the magnetic vector potential. The material behavior is represented by ν, which is a function of **B**. Depending on the material that should be modeled, it can have additional dependence on stress σ, the distance x to the cut edge, or the direction of the magnetic-flux density. Even though the material is more nonlinear compared to the standard isotropic approach, it is still considered to have a scalar value. Especially, for the anisotropy, this is a simplification. Therefore, the named material characteristics can be easily included in every FEM code and the scalar Newton Raphson formulation can be used to consider nonlinear phenomena.

TABLE II
Characteristics of the Simulated PMSM

Rated power P_{N}	30kW
Rated torque T_{N}	100Nm
Rated speed n_{N}	$2860\mathrm{min}^{-1}$
Maximum speed $n_{\max}$	$14000\mathrm{min}^{-1}$
Polepairs	3
Number of phases	3

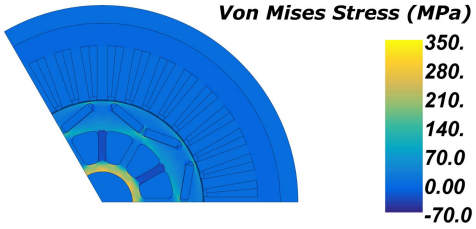

Fig. 4. Stress distribution at maximum speed.

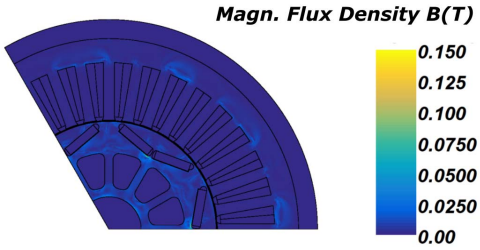

Fig. 5. Flux density difference between stress consideration and without stress consideration.

V. Application on Electric Motor

In this article, a permanent-magnet synchronous machine (PMSM) with buried v-shaped magnets is studied. The shown machine is employed in automotive applications. The machine characteristics are summarized in Table II.

A. Stress Consideration

The mechanical stress that the machine at the maximum speed needs to withstand is shown in Fig. 4. It can be clearly seen that the highest stress occurs in the bridges due to centrifugal forces. A comparison between the simulation with stress consideration and a reference simulation is shown in Fig. 5. Even though the biggest load is in the bridges, the difference between both simulations shows no difference in the bridges, which is because of the high magnetic saturation in these areas. The other areas are more influenced, and the deviation shows compliance with the mechanical stress in the machine. Especially, the fitting shows an impact on the magnetic behavior at the contact of the shaft and the rotor as well as in the stator due to shrinking fitting.

B. Cut-Edge Effect

Next to the mechanical load due to rotation, which is dependent on the speed, and the fitting of the stator, there is always the effect of material degradation caused by the cutting of the laminations. This degradation, which is a function of the distance to the cut edge, is modeled here. The distance is shown in Fig. 6, and the effect takes place if the distance is smaller than x. Evaluating the influence on the flux density

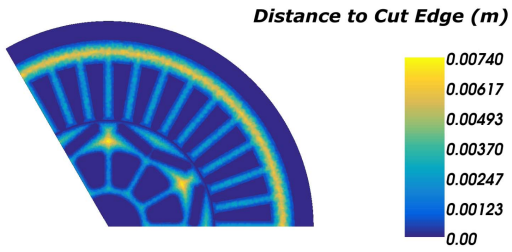

Fig. 6. Distance to cut edge of the steel lamination.

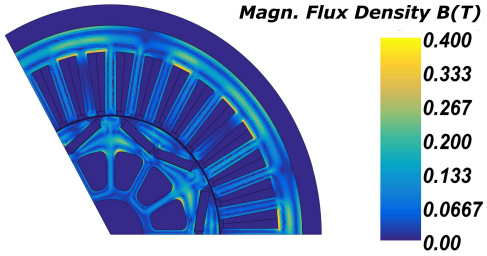

Fig. 7. Influence of the material degradation due to cutting.

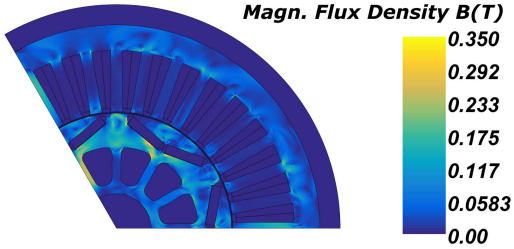

Fig. 8. Influence of the directional dependence on the flux-density distribution compared to reference simulation.

distribution in Fig. 7 clearly indicates the necessity to consider the material degradation. Especially for small machines with many teeth, this effect is not neglectable. This effect is, therefore, antiproportional to the machine's dimension.

C. Directional Dependence

The scalar consideration of directional dependencies is an academic investigation of a nonintrusive anisotropic simulation. For this purpose, the easy direction of the material is set in the x-axis, leading to a preferred direction of the magnetic flux. The resulting difference in the magnetic-flux density distribution is shown in Fig. 8. It is obvious that the flux experiences an anisotropy, which has its maximum in 60°–70° direction. This results in a global deviation of the flux density compared to the reference. Although in reality the influence of ferromagnetic anisotropy can be generally diminished by reasonable stacking of the laminations for general machine designs with distributed windings, the effect is necessary to be modeled in machines with concentrated windings and with segmented stator designs or with grain-oriented material.

VI. Conclusion

Electrical steel sheets, such as M300-50A, which are used for electrical machines, have been measured by means of SST, taking different dependencies into account. Relying on the measured magnetization curves, various material models have been implemented to determine the local magnetizability $J(H)$, with consideration of various dependencies. The implemented approach opens a possibility to calculate the permeability with local distributions of different dependencies. Furthermore, by applying these material models into FE simulation, a comparison study to reference model was carried out. Studies using the corresponding iron losses of measurements and material models are planned to validate the implemented methods.

Acknowledgment

This work was supported by the Deutsche Forschungsgemeinschaft under Grant 373150943, Grant 255713208, and Grant 1487/31-1 through the projects "Vector Hysteresis Modeling of Ferromagnetic Materials," "FOR 1897—Low-Loss Electrical Steel for Energy-Efficient Electrical Drives," and in "SPP 2013—Focused Local Stress Imprint in Electrical Steel as Means of Improving the Energy Efficiency."

References

[1] F. J. G. Landgraf, T. Yonamine, M. Emura, and M. A. Cunha, "Modelling the angular dependence of magnetic properties of a fully processed non-oriented electrical steel," *J. Magn. Magn. Mater.*, vols. 254–255, pp. 328–330, Jan. 2003.

[2] E. Gomes, J. Schneider, K. Verbeken, J. Barros, and Y. Houbaert, "Correlation between microstructure, texture, and magnetic induction in nonoriented electrical steels," *IEEE Trans. Magn.*, vol. 46, no. 2, pp. 310–313, Feb. 2010.

[3] F. Martin, U. Aydin, R. Sundaria, P. Rasilo, A. Belahcen, and A. Arkkio, "Effect of punching the electrical sheets on optimal design of a permanent magnet synchronous motor," *IEEE Trans. Magn.*, vol. 54, no. 3, Mar. 2018, Art. no. 8102004.

[4] M. Cossale, M. Kitzberger, G. Goldbeck, G. Bramerdorfer, D. Andessner, and W. Amrhein, "Investigation and modeling of local degradation in soft magnetic materials," in *Proc. IEEE Energy Convers. Congr. Expo. (ECCE)*, Sep. 2018, pp. 5365–5370.

[5] U. Aydin *et al.*, "Modeling the effect of multiaxial stress on magnetic hysteresis of electrical steel sheets: A comparison," *IEEE Trans. Magn.*, vol. 53, no. 6, Jun. 2017, Art. no. 2000904.

[6] A. J. Moses, N. Derebasi, G. Loisos, and A. Schoppa, "Aspects of the cut-edge effect stress on the power loss and flux density distribution in electrical steel sheets," *J. Magn. Magn. Mater.*, vols. 215–216, pp. 690–692, Jun. 2000.

[7] J. Karthaus, S. Elfgen, and K. Hameyer, "Continuous local material model for the mechanical stress-dependency of magnetic properties in non-oriented electrical steel," *COMPEL—Int. J. Comput. Math. Electr. Electron. Eng.*, vol. 38, no. 1, pp. 1075–1084, 2019.

[8] L. Bernard, B. J. Mailhé, N. Sadowski, N. J. Batistela, and L. Daniel, "Multiscale approaches for magneto-elasticity in device simulation," *J. Magn. Magn. Mater.*, vol. 487, Oct. 2019, Art. no. 165241.

[9] G. Crevecoeur, P. Sergeant, L. Dupre, L. Vandenbossche, and R. Van de Walle, "Analysis of the local material degradation near cutting edges of electrical steel sheets," *IEEE Trans. Magn.*, vol. 44, no. 11, pp. 3173–3176, Nov. 2008.

[10] S. Elfgen, S. Steentjes, S. Böhmer, D. Franck, and K. Hameyer, "Continuous local material model for cut edge effects in soft magnetic materials," *IEEE Trans. Magn.*, vol. 52, no. 5, May 2016, Art. no. 2001304.

[11] R. PremKumar, I. Samajdar, N. N. Viswanathan, V. Singal, and V. Seshadri, "Relative effect(s) of texture and grain size on magnetic properties in a low silicon non-grain oriented electrical steel," *J. Magn. Magn. Mater.*, vol. 264, no. 1, pp. 75–85, 2003.

[12] N. Leuning, S. Steentjes, and K. Hameyer, "On the homogeneity and isotropy of non-grain-oriented electrical steel sheets for the modeling of basic magnetic properties from microstructure and texture," *IEEE Trans. Magn.*, vol. 53, no. 11, Nov. 2017, Art. no. 2002605.

[13] G. Bavendiek, N. Leuning, F. Müller, B. Schauerte, A. Thul, and K. Hameyer, "Magnetic anisotropy under arbitrary excitation in finite element models," *Arch. Elect. Eng.*, vol. 68, no. 2, pp. 455–466, 2019.